Steady State Analysis of Nanofuel Droplet Evaporation

Jude O. Asibor[*] and Osarobo O. Ighodaro

Department of Mechanical Engineering, Faculty of Engineering, University of Benin, 1154, Benin City, Nigeria.

(*) Corresponding author: jude.asibor@uniben.edu

Abstract

The potential for nanofuels as one of the clean sources of energy on account of its enhanced combustion performance coupled with low emissions has been established. Considering the importance of the fuel evaporation phase in the entire combustion process, this work presents an attempt at applying the steady state analysis equations to nanofuel experimental data obtained from the literature in droplet evaporation analysis. The evaporation parameters considered included the rate, constant value (k), the droplet lifetime as well as the D^2 Law response. The extent of applicability of the steady state analysis model equations to nanofuel droplet evaporation was investigated using nanofuel experimental data consisting of ethanol and alumina nanoparticles as well as n-decane and alumina nanoparticles with particle concentration ranging from 0.5-2.5%. The evaporation rate was found to decrease with increasing nanoparticle addition while the droplet lifetime increased marginally, thus validating experimentally obtained result. The nanoparticle inclusion had no effect on the evaporation rate constant value (k) as it remained unchanged throughout the droplet evaporation progression, thus showing adherence to the Classical D^2 Law.

Keywords: D^2 Law, Droplet evaporation, Evaporation rate, Nanofuels.

1. INTRODUCTION

The need for cleaner sources of energy has become a major global issue owing to the effects of global warming and environmental pollution brought about by conventional fossil fuel usage [1]. To this end and coupled with the ever-increasing energy demand, efforts have been made to develop alternative sources of energy (renewable) as well as upgrade the existing traditional hydrocarbon fuels to a level of eco-friendliness and higher efficiencies [2]. One of such discoveries with the potential to meet this need is the Nanofuel. Nanofuels which refers to fuels formed by the mixture of energetic nanomaterials and liquid fuels (mainly gasoline and diesel) have been found to enhance the performance of combustion systems in comparison to the conventional fossil fuels [3-7]. Despite these known and desirable advantages, there is still a dearth of knowledge and understanding on how this nanoparticle inclusion actually brings about this enhanced spray and combustion performance in internal combustion engines (ICEs). While commendable efforts, mainly experimental have been made covering areas such as thermo-physical property analysis, combustion sub-processes, nanoparticle parameter analysis, use of surfactants among others [8-14], not much effort has been done in the area of spray behaviour analysis, atomization process, droplet study and evaporation [15-17].

2. SPRAY DROPLET EVAPORATION

The evaporation behaviour of a droplet in an oxidizing environment provides insight into the behaviour of the overall spray [17]. Evaporation involves the process of simultaneous heat, mass and momentum transfer. While the heat transfer to the droplet from the environment involves the processes of conduction and convection, the vapor transfer from the droplet into the surrounding environment involves the

processes of convection and diffusion. Lefebvre and McDonell [18] identified the factors affecting the overall evaporation rate to include the ambient temperature, pressure, transport properties, the spray properties such as the temperature, droplet size, liquid density, viscosity, volatility as well as the relative velocity between the drops and the surrounding environment.

With emphasis on fuel droplet evaporation, Emekwuru [17] as well as Lefebvre and McDonell [18] explained that there were two mechanisms of combustion; the heterogeneous combustion in which case a diffusion flame surrounds the fuel droplet as it evaporates, and the more common homogeneous or pre-mixed combustion in which the fuel droplet is vaporised completely and mixes with the surrounding air to form an air-fuel mixture before combustion sets in on the attainment of the ignition temperature. With regards to this pre-mixed combustion mode, it has been observed that the droplet evaporation process consists of two phases; the unsteady state and steady state evaporation. In the unsteady phase (heat-up period), the bulk of the heat transferred to the droplet is used in raising the fuel temperature to its wet-bulb temperature, hence very little evaporation or change in droplet size can be observed. Lefebvre and Ballal [19] reports that this phase is commonly observed under conditions of high ambient pressures and temperature in which case it is not neglected during analysis.

On completion of the heat-up period, the steady state evaporation phase begins in which the heat and mass transfer between the droplet and the surrounding gases occur. This process is characterised by a reduction of the droplet size with time. The relationship between this rate of droplet size reduction with respect to time is what is commonly referred to as the D^2 Law. This law attributed to Godsave states that during droplet evaporation, the rate of change of the square of the droplet diameter is directly proportional to the change in time [18]. This relationship is presented in equation (1).

$$D_0^2 - D^2 = \lambda t \qquad (1)$$

Where, D_0 is the initial droplet diameter, D is the instantaneous droplet diameter at a given time, λ is the evaporation constant (mm^2/s) and t is the time (s).

It is important to note that in real-life situations, fuel droplets do not necessarily attain steady state on account of the many complex parameters at play during the evaporation process, hence a term known as 'quasi-steady state' has been applied by various researchers [18]. However, for the purpose of numerical analysis, characterisation droplet studies as well as system performance predictions, the steady state evaporation analysis is still of utmost relevance today. The application of the steady state analysis method is based on some assumptions which are given as follows [18];

• spherical droplet shape.
• liquid fuel with defined boiling point.
• negligible heat transfer by radiation.

Several droplet and spray studies involving experimental and numerical analysis as well as models have been developed using various liquids as a means of understanding, predicting and optimizing system performance. Some of these research attempts as it relates to conventional fuels, nanofluids as well as nanofuels are briefly discussed in the following sections.

2.1. Conventional Fossil Fuels

Kadota and Hiroyasu [20] investigated the effect of ambient condition (high temperature and pressure environment) on the evaporation of n-heptane and developed models for predicting temperature and droplet sizes during the evaporation process. Lefebvre and Chin [21] applied the steady state analysis method in evaluating the droplet evaporation characteristics of five selected fuels (n-heptane, aviation gasoline, JP4, JP5 and diesel oil (DF2)) under no flow conditions (quiescent). The result of this

investigation showed that temperature and pressure were key influencers of the evaporation rate while the obtained evaporation rate constant value was consistent with experimentally obtained values thus showing the robustness of the steady state method. Verwey and Birouk [22] investigated the effect of the droplet size on the evaporation rate in a turbulent environment using n-heptane and n-decane which are gasoline and diesel surrogates respectively. They reported that in both fuel cases, the evaporation process followed the D^2 law and the evaporation rate increased with increase in the turbulent intensity and droplet size.

Several analytical models have been developed to study and predict spray evaporation with one of the earliest (Classical droplet vaporisation model) being the D^2 Law Model with its assumptions of spherical symmetrical droplets and no convection [23]. This model which measures the mass transfer rate, $\dot{m}_f$ (kg/s) is presented in equation (2).

$$\dot{m}_f = -2\pi D_0 \rho D_{sm} \ln(1 + B_m) \qquad (2)$$

where, ρ is the density (kg/m^3), D_{sm} is the mass diffusion coefficient and B_M is the Spalding mass transfer number.

Dent and Mehta [24] applied a modified version of the D^2 Law Model by including the effect of convection as well as a correlation of Nusselt number, Reynolds number and Prandtl number. Kim and Sung [25] investigated the effect of ambient pressure on the evaporation rate of n-heptane and reported a direct relationship between the droplet lifetime and pressure at low temperature and an inverse relation at high temperature. This dependence on pressure was also corroborated by Kitano et al. [26] using a 3D numerical simulation model. They also reported a droplet evaporation acceleration brought about by natural convection. A comprehensive review of droplet eva-poration studies has been presented by various researchers covering areas such as droplet heating models, turbulence effects on evaporation rate as well as sessile and suspended drop evaporation [17, 27-30].

2.2. Nanofluids and Nanofuels

Efforts have been made in the droplet study of nanofluids especially in regards to sessile droplets and how the nanoparticles impact on the wettability and evaporation dynamics. Chen et al. [31] carried out extensive experimental study on the effect of nanoparticle inclusion on heat transfer and fuel droplet evaporation using laponite, Fe_2O_3 and silver nanoparticles in deionised water. They reported varying evaporation constant (k) values for the different nanoparticles as the evaporation progressed. Sefiane and Bennacer [32] investigated the effect of aluminium nanoparticle inclusion on the evaporation of sessile ethanol droplet and reported a reduction in the evaporation rate. According to them, this was as a result of the increased viscosity brought about by the nanoparticle inclusion which slowed down the internal fluid motion from the droplet core to the surface during the evaporation process. While a reduction in evaporation rate was reported for the droplet study, in the case of the spray analysis, the nanoparticle inclusion brought about an increase in the overall evaporation rate. This discrepancy in result could be linked to other factors that come into play in the spray analysis such as droplet collision effects, relative velocity between the spray droplets and the surrounding environment as well as prevailing ambient conditions. A similar result of droplet evaporation rate reduction was reported by Gerken et al. [33] for a droplet suspended in a pendant manner.

With regards to the D^2 law adherence, Wei et al. [34] using a model showed that the nanofluid evaporation deviated from the classical D^2 law. This they attributed to the increased particle inclusion on the droplet surface as the evaporation progressed thus hindering effective surface area for heat and mass transfer. While most of the efforts at nanofuel droplet study have been carried out under ambient

and low temperature conditions, attempts have also been made in higher ambient temperature investigations. Results from these investigations showed adherence to the D^2 law of the evaporation process coupled with increase in the evaporation rate brought about by the decomposition of the surfactant at elevated temperatures [35]. The steady state droplet evaporation progression at elevated temperature was explained to consist of three periods; the liquid dominant, the dry-out and the nanoparticle strain periods. While the concept of bubble formation and micro-explosion as well as shell formation on evaporation completion was also reported [36-38].

In Gan and Qiao [16], the evaporation characteristics of two nanofuels, aluminium nanoparticles in ethanol and aluminium nanoparticles in n-decane were investigated under natural and forced convections. For both fuel cases, they reported a departure from the D^2 law under conditions of low temperatures and natural convection. They attempted to link this deviation to the phenomenon of particle aggregation within the droplet during the evaporation process by developing a particle aggregation model based on the population balanced equation. They also reported a decrease in the evaporation rate with increase in particle concentration under ambient conditions. Since only steady state evaporation process was considered in this experimental work and considering the versatility of the classical D^2 law, there is need to apply the steady state evaporation analysis equations as a means of validating these obtained results and also investigating the extent of its application to nanofuels.

To achieve this, experimental data from the literature will be applied to the steady state equations. The evaporation characteristics that will be considered with regards to the effect of nanoparticle addition include the evaporation rate, the evaporation constant value, droplet lifetime, adherence to the D^2 law as well as effect of initial droplet concentration.

3. METHODOLOGY

Two nanofuels: ethanol + aluminium nanoparticles and n-decane + aluminium nanoparticles were analysed using the steady state equations. Aside the need for robustness of obtained results, the use of these two fuels also offers some insights on probable effects of the type of base fuel applied. This study is broken down into three major sections with the first two sections covering the nanoparticle inclusion effect on the droplet evaporation parameters for the two fuels; while the third section will concern itself with the effect of the initial particle concentration on the evaporation rate.

3.1. Ethanol + Aluminium Nanoparticle Droplet Analysis

Single droplets of the same diameter size, D_0 =1mm but with different nanoparticle concentrations, 0.5% and 2.5% by weight were considered at ambient temperature, T_∞ of 300K [16].

A. Effect on Evaporation Rate and Evaporation Constant

The reference temperature, T_r for the analysis was obtained using equation (3) [18]

$$T_r = T_s + \frac{T_\infty - T_s}{3} \tag{3}$$

Taking the fuel surface temperature, T_s = 288.6K, then $T_r = 292.4K$, the evaporation rate, λ_{st} is given by equation (4) as obtained from Lefebvre and McDonell [18]

$$\lambda_{st} = \frac{8 \times k_g \times \ln(1 + B_m)}{Cp_g \times \rho_F} \tag{4}$$

Where, Cp_g is the fuel-air mixture specific heat (kJ/kg-K), k_g is the fuel-air mixture thermal conductivity (kJ/m-s-K), ρ_F is the liquid fuel density and B_M is the Spalding mass transfer number given by equation (5) below as obtained from Siewert [39].

$$B_M = \frac{Y_{Fs}}{1 - Y_{Fs}} \tag{5}$$

where Y_{FS} is the fuel mass fraction at the droplet surface given by equation (6)

$$Y_{FS} = \left[1 + \left(\frac{P}{P_{FS}} - 1 \right) \frac{M_A}{M_F} \right]^{-1} \tag{6}$$

where, P is the ambient pressure, 101.3kPa, M_A is the molecular weight of air, 28.97g/mol

M_F is the molecular weight of ethanol, 46g/mol.

The fuel vapour pressure at the drop surface, P_{FS} was obtained using equation (7)[39].

$$P_{FS} = exp\left(a - \frac{b}{c+T_s-273}\right) \qquad (7)$$

For ethanol, a =8.04494, b = 1554.3 and c = 222.65 [39]

On substituting these values into equations (6) and (7),

$P_{FS} = 4.5773\ kPa$, $Y_{FS} = 0.0699$

The mass fractions at the reference temperature for the fuel, Y_{FR} and air, Y_{AR} were thus obtained from equations (8) and (9) respectively [18].

$$Y_{Fr} = \frac{2}{3}Y_{Fs} \qquad (8)$$

$$Y_{Ar} = 1 - Y_{Fr} = 1 - \frac{2}{3}Y_{Fs} \qquad (9)$$

Note that under steady state conditions, $B_M = B_T = B$, where B_T is the Heat Transfer Number [18].

Having obtained the mass fractions and taking boiling point temperature of ethanol, $T_{bn} = 352K$ and the density of ethanol at 288.6k, $\rho_{F0} = 796\ kg/m^3$ [39], the fuel-air mixture thermal conductivity, k_g as well as the mixture's specific heat, Cp_g, were obtained using equations (10) to (14) as follows[18].

$$k_g = Y_{Ar}(k_A\ at\ T_r) + Y_{Fr}(k_v\ at\ T_r) \qquad (10)$$

Where, k_A is the thermal conductivity of the ambient air, 0.03855 J/msK. The thermal conductivity of the fuel vapour, k_V is obtained as follows

$$k_v = 10^{-3}[13.2 - 0.0313(T_{bn} - 273)](\frac{T}{273})^n \qquad (11)$$

$$n = 2 - 0.0372(\frac{T}{T_{bn}})^2 \qquad (12)$$

The specific heat of the air-fuel mixture was obtained from equation (13)

$$Cp_g = Y_{Ar}(Cp_A\ at\ T_r) + Y_{Fr}(Cp_v\ at\ T_r) \qquad (13)$$

$$Cp_v = (363 + 0.467T)(5 - 0.001\rho_{F0}) \qquad (14)$$

$k_g = 0.025\ J/msK$, Cp_g= 1055.27J/kgK

On substituting these obtained values into equation (4), the equation for the evaporation rate as a function of the liquid fuel density was obtained as follows,

$$\lambda_{st} = \frac{1.371}{\rho_F} \qquad (15)$$

Taking the densities of the ethanol droplets with 0.5% nano-Al and 2.5% nano-Al to be 792.5kg/m³ and 803.8kg/m³ respectively [32], the value of the evaporation constants which depict the evaporation rates was thus obtained.

For the ethanol droplets with 0.5% nano-Al, $\lambda_{st} = 0.00173 mm^2/s$,

For the ethanol droplets with 2.5% nano-Al, $\lambda_{st} = 0.00171 mm^2/s$

B. D² Law Analysis

The D² Law was applied using following equation

$$D^2 = D_0^2 - \lambda t \qquad (1)$$

On dividing through equation (1) and substituting the obtained values of evaporation constants for the 0.5% and 2.5% nano-Al droplets, equations (16) and (17) were obtained respectively,

$$D^2/D_0^2 = 1 - 0.00173\ t/D_0^2 \qquad (16)$$

$$D^2/D_0^2 = 1 - 0.00171\ t/D_0^2 \qquad (17)$$

On plotting these equations with their respective experimental results, the D² Law behaviours for the respective droplet evaporation process was thus obtained as shown in Figures 4 and 5.

C. Effect on Droplet Lifetime

The steady state droplet lifetime, t_e for both cases of nanoparticle concentration was obtained on re-arranging equation (1) with time (t_e) as the subject and the instantaneous diameter, D equated to zero to indicate evaporation completion. A constant term of 1.5 was assumed to represent the effects of weak convective forces [39] as presented in equation (18).

$$t_e = \frac{D_0^2}{1.5 \times \lambda_{st}} \qquad (18)$$

3.2. N-decane + Aluminium Nanoparticle Droplet Analysis

In carrying out this analysis, same conditions as those applied for the ethanol case study were used with the reference temperature, $T_r = 292.4K$ and the fuel surface temperature, $T_s = 288.6K$. On applying the steady state analysis equations as presented in section 3.1, the evaporation rates were obtained.

For the ethanol droplets with 0.5% nano-Al, $\lambda_{st} = 0.00104mm^2/s$,

For the ethanol droplets with 2.5% nano-Al, $\lambda_{st} = 0.001033mm^2/s$

From these values, the corresponding D^2 Law equations were obtained as follows,

$$D^2/D_0^2 = 1 - 0.00104\, t/D_0^2 \qquad (19)$$

$$D^2/D_0^2 = 1 - 0.001033\, t/D_0^2 \qquad (20)$$

Also, the steady state droplet lifetime, t_e for both cases of nanoparticle concentration was obtained on substituting the required obtained values into equation (18).

3.3. Determination of the Effect of Initial Nanoparticle Concentration on the Evaporation Rate

The same analysis conditions as in section 3.1 was applied aside the fuel composition given in Table 1. From section 3.1, equation (15) for the evaporation rate as a function of the liquid fuel density for ethanol + nano Al has been obtained as,

$$\lambda_{st} = \frac{1.371}{\rho_F} \qquad (15)$$

Using the data in Table 1, this function was then plotted in order to obtain the required result.

Table 1. *Nanofuel Data [32]*

Fuel composition : Aluminum nanoparticles in ethanol	
Nanoparticle concentration (weight %)	Density (kg/m^3)
0	789.7
3.5	809.5
5.1	819.5
6.8	829.5

4. RESULTS AND DISCUSSION

4.1. Effect on Evaporation Rate and Evaporation Constant

The obtained results were then plotted and compared to the experimental results of Gan and Qaio [16] as presented in Figures 1 and 2. Figures 1 and 2 show the plots of evaporation constant (k) vs t/D^2 for aluminiun nanoparticle (Al NP) in ethanol and n-decane respectively. As shown in Figures 1 and 2, the obtained steady state result values of the evaporation constant (k) does not vary with time for both nanoparticle (NP) concentration scenarios in both base fuel cases. This expected response which is due to the time independent structure of the equations applied in the steady state analysis does not agree with the experimental results Gan and Qaio [16] in which the k value is continuously varying and reducing with time. A phenomenon which they explained was as a result of the aggregation of the nanoparticles as the evaporation process progressed. This freshly formed aggregates impedes the fluid motion within the droplet thus slowing down the evaporation rate.

This obtained result does not also agree with the transition concept of Chen *et al.* [31] in which the k value is expected to change at what they referred to as critical time on account of the relative nanoparticle concentration increasing as the evaporation progressed. Since the steady state model is purely linear and does not include particle dependent parameters which explains its marked discrepancy with other experimentally obtained results, it therefore fails in providing adequate prediction of the evaporation constant value response brought about by particle inclusion.

However, it is important to note that while it fails in the evaporation constant value analysis, it succeeds in predicting particle concentration effect on the evaporation rate. This can be clearly observed in ethanol (Figure 1) and n-decane (Figure 2) base fuel cases as the 0.5% nano-Al gives a higher evaporation

rate compared to the 2.5% nano-Al though this difference is very small and almost negligible. This smallness in the magnitude is due to the analysis conditions especially in regards to the low ambient temperature. Under operational combustion chamber conditions, the effect of the particle inclusion is expected to be more significant as the phenomenon of bubble formation as well as micro-explosions will then set in coupled with an overall higher rate of evaporation irrespective of the nanoparticle concentration.
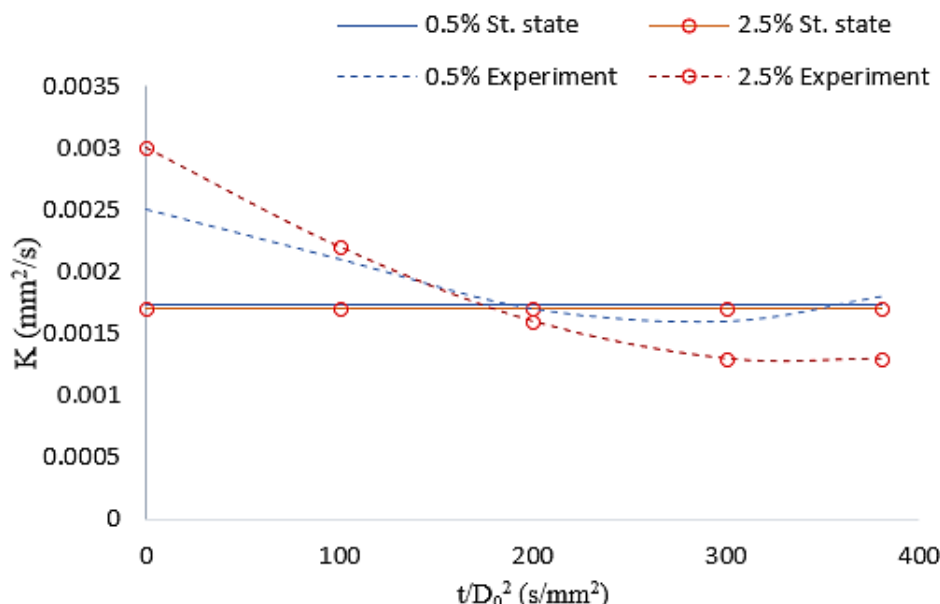

Figure 1. *Experimental and Steady state results comparison for ethanol with Al NP droplet evaporation.*
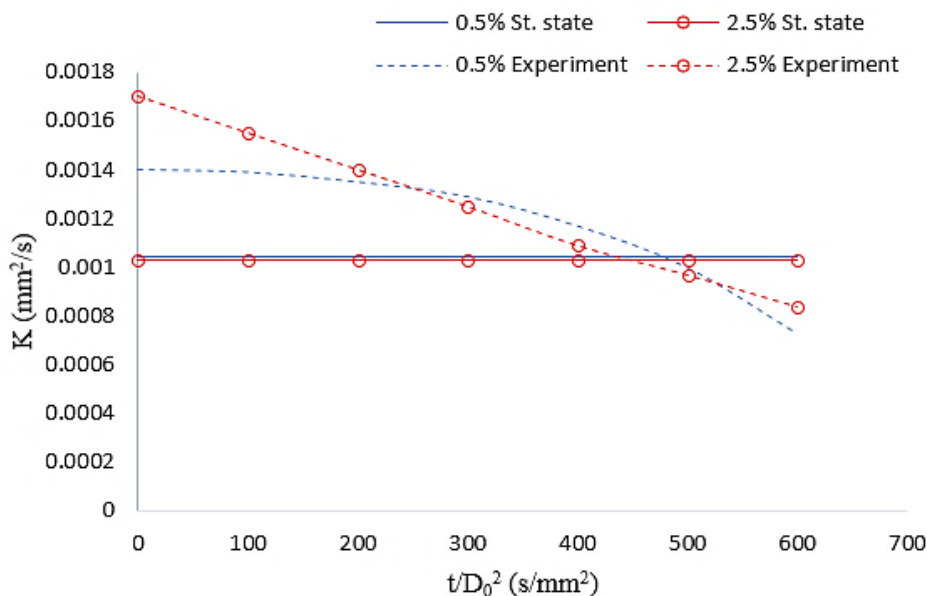

Figure 2. *Experimental and Steady state results comparison for n-decane with Al NP droplet evaporation.*

With regards to Figures 1 and 2, it can be observed that for steady state results, the higher evaporation rate obtained at the 0.5% nanoparticle concentration is maintained throughout the evaporation process. In the case of the experimental

results, there is a switch in the evaporation rate trend with the 0.5% loading accounting for the higher evaporation rate as the process progresses. This trend which clearly agrees with the steady state model results, though on a different scale finds its explanation in the particle aggregation phenomenon which involves the increase in the relative concentration of the nanoparticle as the liquid phase of the droplet is being vaporised. This increased concentration of the nanoparticles (now aggregated) impedes the subsequent flow of the liquid from the core towards the droplet surface, thus reducing the rate of the evaporation.

From the foregoing and within the analysis conditions, the steady state model quantitatively predicts the effect of the particle inclusion on the evaporation rate. This reduction in evaporation rate with increase in nanoparticle concentration using the steady state model equations is more clearly captured on applying the experimental data of Sefiane and Bennacer [32] presented in section 3.3 with the obtained result shown in Figure 3 and discussed in section 4.2.

On plotting the function obtained in equation (36) using the data from Table 1, the result shown in Figure 3 was obtained. Figure 3 shows the obtained plot of the evaporation rate against the nanoparticle (NP) concentration. As shown in the figure, the evaporation rate decreases with increasing initial NP concentration.
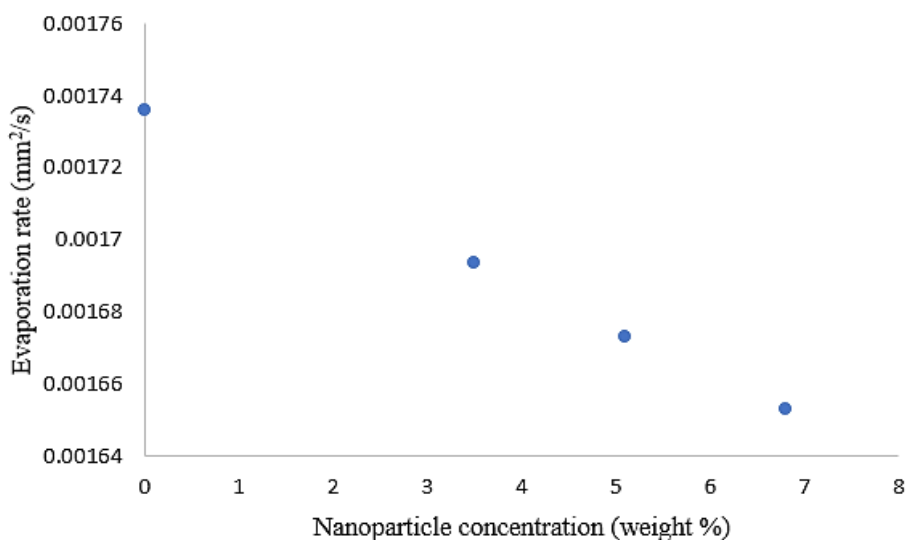

Figure 3. *Obtained plot of the variation of the evaporation constant with Initial NP concentration*

4.2. Determination of the Effect of Initial Nanoparticle Concentration on the Evaporation Rate

While Figures 1 and 2 give details of the time progression of the evaporation process with little information on the influence of the particle density on the evaporation rate, Figure 3 clearly presents the relationship between the evaporation rate and the nanoparticle concentration obtained using the steady state model equations for ethanol and aluminium nanoparticles under the analysis conditions presented in section 3.3. This obtained result which is also in agreement with experimentally obtained results also finds its explanation in the particle aggregation and particle impediment to fluid motion concept already discussed in the previous section.

Figures 1 and 2 show higher range of k values for the ethanol-based fuel compared to the n-decane based fuel. This is as a result of the higher volatility and lower boiling point temperature of ethanol compared to n-decane thus bringing to the fore the complementary influence of the

base fuel properties in determining the evaporation rate progression.

4.3. D^2 Law Analysis

As presented in Figures 4 and 5, the evaporation of the respective nanofuel combinations using the steady state analysis model and applied conditions follows the D^2 Law. This is expected as the equation applied in the plot is a linear one, hence it gave a linear output. Though it does not exactly agree with the experimental reference study [16] as shown in the figures, it does fairly well in giving an approximate representation of the evaporation rate progression as it concerns the droplet size reduction.
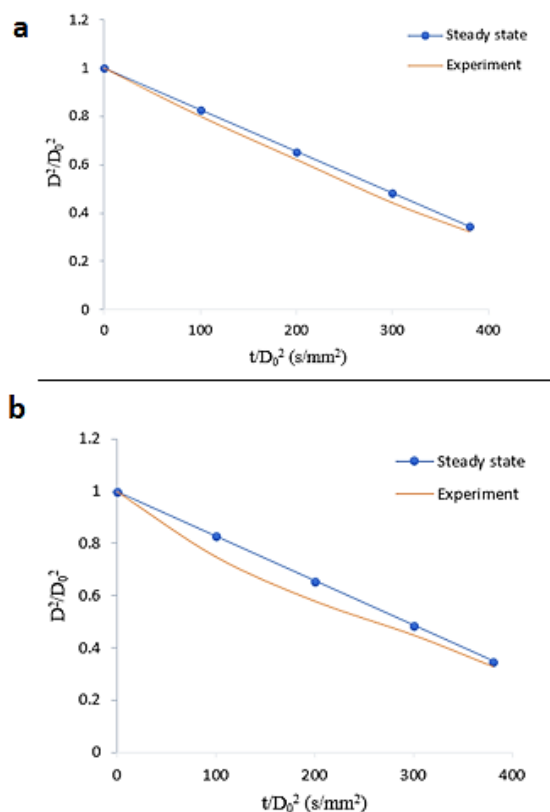

Figure 4. Evaporation of ethanol droplets under natural convection at 300K with (a) 0.5% nano- Al. (b) 2.5% nano- Al.

Considering the ambient conditions of analysis, it is understandable that though the particle inclusion reduced the evaporation rate as discussed in preceeding sections, it does not seem to have affected the droplet size reduction progression. This is mainly as a result of the low ambient

temperature which ensures that the phenomena of bubble formation and micro-explosion usually associated with elevated ambient temperature does not occur, hence, the liquid phase of the droplet evaporated in a linear manner as presented in the figures though at a lower evaporation rate. Another key probable factor that could be responsible for this discrepancy in result is hinged on the assumptions associated with the steady state analysis model which obviously are not ignored in the experimental study.

4.4. Effect on Droplet Lifetime

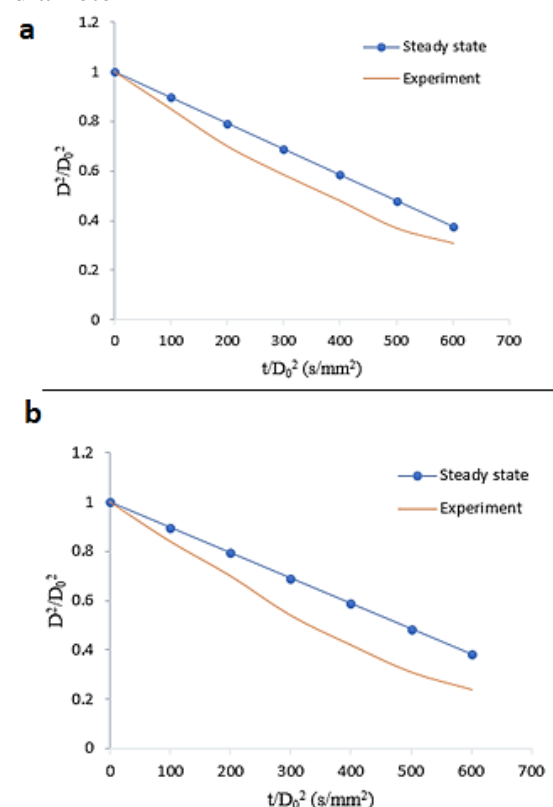The results obtained on substitution of the required values of initial droplet diameter

Figure 5. Evaporation of n-decane droplets under natural convection at 300K with (a) 0.5% nano- Al (b) 2.5% nano- Al.

and liquid fuel density into equation (18) showed that while the 0.5% nano-Al ethanol droplet had a droplet lifetime of 385.33s, the 2.5% nano-Al droplet had a higher droplet lifetime of 390.86s. In the case of the n-decane + aluminium nanoparticle combination, the 0.5%

concentration gave a droplet lifetime of 641.03s while the 2.5% nano-Al droplet had a higher droplet lifetime of 645.36s.

From these results, it can be seen that the droplet lifetime increases with increase in the nanoparticle concentration, though in a fairly small amount. This trend is directly linked to the lower evaporation rate of the higher nanoparticle droplet as it will thus take a longer time for the liquid to be completely evaporated. It is also important to note that the base fuel boiling point temperature plays a key role in determining the droplet lifetime. This explains the longer droplet lifetime of the n-decane based fuel compared to the ethanol-based fuel.

5. CONCLUSIONS

- Using the steady state analysis method, the evaporation rate has been found to decrease with increasing nanoparticle addition, thus validating experimentally obtained result.
- The nanoparticle inclusion had no effect on the evaporation constant value (k).
- Steady state analysis cannot be applied to transient droplet evaporation rate analysis.
- The evaporation process has been found to follow the Classical D^2 Law.
- The droplet lifetime has been found to increase marginally with increasing nanoparticle addition.

CONFLICT OF INTEREST

There is no conflict of interest among the authors of this research article.

REFERENCES

1. National Geographic., (2018). "*Air Pollution Causes, Effects, and Solutions*". Retrieved from https://www.nationalgeofuhic.com/environment/global-warming/pollution/ [Accessed 20 Sep. 2018].
2. Saxena, V., Kumar, N., Saxena, V., (2017). "A comprehensive review on combustion and stability aspects of metal nanoparticles and its additive effect on diesel and biodiesel fuelled C.I. engine", *Renewable and Sustainable Energy Reviews*, 70: 563-588.
3. Mehta, R., Chakraborty, M., Parikh, P., (2014). "Nanofuels: Combustion, Engine Performance and Emissions", *Fuel,* 120: 91-97.
4. Shaafi, T., Velraj, R., (2015). "Influence of Alumina Nanoparticles, Ethanol and Isopropanol Blend as Additive with Diesel–Soybean Biodiesel Blend Fuel: Combustion, Engine Performance and Emissions", *Renewable Energy,* 80: 655-663.
5. D'Silva, R., Binu, K., Bhat, T., (2015). "Performance and Emission Characteristics of a C.I. Engine Fuelled with Diesel and TiO$_2$ Nanoparticles as Fuel Additive", *Materials Today: Proceedings,* 2 (4-5): 3728-3735.
6. Sungur, B., Topaloglu, B., Ozcan, H., (2016). "Effects of Nanoparticle Additives to Diesel on The Combustion Performance and Emissions of a Flame Tube Boiler", *Energy,* 113: 44-51.
7. Khond, V., Kriplani, V., (2016). "Effect of Nanofluid Additives on Performances and Emissions of Emulsified Diesel and Biodiesel Fueled Stationary CI Engine: A Comprehensive Review", *Renewable and Sustainable Energy Reviews,* 59: 1338-1348.
8. Gumus, S., Ozcan, H., Ozbey, M., Topaloglu, B., (2016). "Aluminium Oxide and Copper Oxide Nanodiesel Fuel Properties and Usage in A Compression Ignition Engine", *Fuel,* 163: 80-87.
9. Kannaiyan, K., Sadr, R., (2017). "The Effects of Alumina Nanoparticles as Fuel Additives on The Spray Characteristics of Gas-To-Liquid Jet Fuels", *Experimental Thermal and Fluid Science,* 87: 93-103.
10. Shariatmadar, F., Pakdehi, S. (2017). "Synthesis and Characterization of Aviation Turbine Kerosene Nanofuel Containing Boron Nanoparticles", *Applied Thermal Engineering,* 112: 1195-1204.
11. Lenin, M., Swaminathan, M., Kumaresan, G., (2013). "Performance and Emission Characteristics of A DI Diesel Engine with A Nanofuel Additive", *Fuel,* 109: 362-365.
12. Tanvir, S., Qiao, L., (2012). "Surface Tension of Nanofluid-Type Fuels Containing Suspended Nanomaterials", *Nanoscale Research Letters,* 7 (1): 226.
13. Gupta, M., Singh, V., Kumar, R., Said, Z., (2017). "A Review on Thermophysical Properties of Nanofluids And Heat Transfer Applications", *Renewable and Sustainable Energy Reviews,* 74: 638-670.

14. Suganthi, K., Rajan, K., (2017). "Metal Oxide Nanofluids: Review of Formulation, Thermo-Physical Properties, Mechanisms, And Heat Transfer Performance", *Renewable and Sustainable Energy Reviews,* 76: 226-255.

15. Asibor J. O., Emekwuru N., Pandey K., Basu S., (2018). "*Characterization of the Spray Cone Angles of Fuels with Nanoparticle Additives*", Proceedings of the 14th Triennial International Conference on Liquid Atomization and Spray Systems, Chicago, IL, USA.

16. Gan, Y., Qiao, L., (2011). "Evaporation Characteristics of Fuel Droplets with The Addition of Nanoparticles Under Natural and Forced Convections", *International Journal of Heat and Mass Transfer,* 54 (23-24): 4913-4922.

17. Emekwuru N. G., (2018). "Nanofuel Droplet Evaporation Processes", *Journal of the Indian Institute of Science*. https:// doi.org/10.1007/s41745-018-0092-2.

18. Lefebvre, A., McDonell, V., (2017). "*Atomization and Sprays",* CRC Press LLC, Boca Raton.

19. Lefebvre, A., Ballal, D., (2010). "*Gas turbine combustion*", Taylor & Francis, Boca Raton.

20. Kadota, T., Hiroyasu, H., (1976). "Evaporation of a Single Droplet at Elevated Pressures and Temperatures: 2nd Report, Theoretical Study", *Bulletin Of JSME*, 19(138): 1515-1521.

21. Lefebvre, A., Chin, J., (1983). "Steady-state evaporation characteristics of hydrocarbon fuel drops", *AIAA Journal*, *21*(10): 1437-1443.

22. Verwey, C., Birouk, M., (2017). "Experimental investigation of the effect of droplet size on the vaporization process in ambient turbulence", *Combustion and Flame*, 182: 288-297.

23. Payri, F., Benajes, J., Tinaut, F., (1988). "A Phenomenological Combustion Model for Direct-Injection, Compression-Ignition Engines", *Applied Mathematical Modelling,* 12 (3): 293-304.

24. Dent, J., Mehta, P., (1981). "Phenomenological Combustion Model for A Quiescent Chamber Diesel Engine", *SAE Technical Paper*, 811235.

25. Kim, H., Sung, N., (2003). "The effect of ambient pressure on the evaporation of a single droplet and a spray", *Combustion and Flame*, 135(3): 261-270.

26. Kitano, T., Nishio, J., Kurose, R., Komori, S., (2014). "Effects of ambient pressure, gas temperature and combustion reaction on droplet evaporation", *Combustion and Flame*, 161(2): 551-564.

27. Sazhin, S., (2017). "Modelling of fuel droplet heating and evaporation: Recent results and unsolved problems", *Fuel*, 196: 69-101.

28. Birouk, M., Gokalp, I., (2006). "Current status of droplet evaporation in turbulent flows", *Progress in Energy and Combustion Science*, 32(4): 408-423.

29. Erbil, H., (2012). "Evaporation of pure liquid sessile and spherical suspended drops: A review", *Advances in Colloid and Interface Science*, 170(1-2): 67-86.

30. Abramzon, B., Sirignano, W., (1989). "Droplet vaporization model for spray combustion calculations", *International Journal of Heat and Mass Transfer*, 32(9): 1605-1618.

31. Chen, R., Phuoc, T., Martello, D., (2010). "Effects of nanoparticles on nanofluid droplet evaporation", *International Journal of Heat and Mass Transfer*, 53(19-20): 3677-3682.

32. Sefiane, K., Bennacer, R., (2009). "Nanofluids droplets evaporation kinetics and wetting dynamics on rough heated substrates", *Advances in Colloid and Interface Science*, 147-148: 263-271.

33. Gerken, W., Thomas, A., Koratkar, N., Oehlschlaeger, M., (2014). "Nanofluid pendant droplet evaporation: Experiments and modelling", *International Journal of Heat and Mass Transfer*, 74: 263-268.

34. Wei, Y., Deng, W., Chen, R., (2016). "Effects of insoluble nano-particles on nanofluid droplet evaporation", *International Journal of Heat and Mass Transfer*, 97: 725-734.

35. Javed, I., Baek, S., Waheed, K., (2013). "Evaporation characteristics of heptane droplets with the addition of aluminum nanoparticles at elevated temperatures", *Combustion and Flame*, 160(1): 170-183.

36. Javed, I., Baek, S., Waheed, K., Ali, G., Cho, S., (2013). "Evaporation characteristics of kerosene droplets with dilute concentrations of ligand-protected aluminium nanoparticles at elevated temperatures", *Combustion and Flame*, 160(12): 2955-2963.

37. Javed, I., Baek, S., Waheed, K., (2014). "Effects of dense concentrations of aluminium nanoparticles on the evaporation behaviour of kerosene droplet at elevated temperatures: The phenomenon of micro-explosion", *Experimental Thermal and Fluid Science*, 56: 33-44.

38. Gan, Y., Lim, Y., Qiao, L., (2012). "Combustion of Nanofluid Fuels with The Addition of Boron and Iron Particles at Dilute and Dense Concentrations", *Combustion and Flame,* 159 (4): 1732-1740.

39. Siewert, R., (2007). "A Phenomenological Engine Model for Direct Injection of Liquid Fuels, Spray Penetration, Vaporization, Ignition Delay and Combustion", *SAE Technical Paper Series,* 2007-01-0673.